Astron. Astrophys. 347, 957–966 (1999)

ASTRONOMY
AND
ASTROPHYSICS

Deuterium in the Sagittarius B2 and Sagittarius A galactic center regions

T. Jacq[1], **A. Baudry**[1], **C.M. Walmsley**[2], **and P. Caselli**[2]

[1] Observatoire de l'Université de Bordeaux I, B.P. 89, F-33270 Floirac, France
[2] Osservatorio Astrofisico di Arcetri, Largo E. Fermi 5, I-50125 Firenze, Italy

Received 23 December 1998 / Accepted 10 May 1999

Abstract. We report IRAM 30-m observations of DCN and DCO^+ towards the galactic center molecular clouds Sgr B2 and Sgr A. We compare our results with simultaneous measurements of $H^{13}CN$ and $HC^{18}O^+$ in order to derive estimates of the [DCN]/[HCN] and [DCO^+]/[HCO^+] abundance ratios. We mapped Sgr B2 in DCN(2-1) and DCN(3-2) and we compared $HC^{15}N$ with DCN for one position of our maps. The uncertainties in such measurements turn out to be large, due to optical depth effects, in the case of $H^{13}CN$, and, in the case of Sgr B2, due to the strong foreground absorption in $H^{13}CN$, $HC^{15}N$ and $HC^{18}O^+$. Taking these effects into account, we conclude that [DCN]/[HCN] towards the molecular ridge in Sgr B2 is $1.3\,10^{-4}$ (uncertain by a factor 2) and towards the Sgr A molecular cloud is $< 6\,10^{-4}$. Towards Sgr B2, we also estimate [DCO^+]/[HCO^+] to be $2\,10^{-4}$ again with a factor of 2 uncertainty. We have carried out model calculations to estimate the amount of deuterium enhancement in these species in these clouds. We find, for temperatures between 40 and 120 K, that one expects D to be enhanced in DCN in the galactic center by a factor between 12 and 140 over the actual ratio of [D/H]. The corresponding enhancement for DCO^+ would be between 23 and 460. Based on these results, we conclude that the ratio of [D/H] in the Sgr B2 cloud is $5\,10^{-6}$ with a factor of 10 uncertainty. This result, while it has large uncertainty, suggests that deuterium is roughly one order of magnitude less abundant in the galactic center than in the solar neighbourhood. We briefly discuss possible consequences of this for the stellar initial mass function in the galactic center.

Key words: ISM: abundances – ISM: molecules – Galaxy: center – radio lines: ISM

1. Introduction

The distribution of the D/H abundance ratio in the galactic disk is extremely poorly known. In the solar neighborhood, measurements of interstellar atomic deuterium Lyman lines towards early type stars have allowed a relatively precise determination of the deuterium abundance (e.g. Boesgaard & Steigman (1985), Pasachoff & Vidal-Majar (1989)). The values derived vary between $8\,10^{-6}$ and $3\,10^{-5}$. They are consistent with the recent HST observations of the D Lyman alpha line (Linsky et al., 1993) yielding D/H $\approx 1.7\,10^{-5}$ in the local medium. In other regions of the Galaxy, there is very little direct evidence. Towards the HI clouds in the galactic center, Lubowich et al. (1989) have used measurements of the 327 MHz hyperfine transition of atomic deuterium to determine an upper limit of $4.3\,10^{-3}$ for the ratio of deuterium to hydrogen atoms. Similar measurements made towards Cas A gave an upper limit of about $6\,10^{-4}$ (Heiles et al., 1993). In such regions however, D may be in HD, so the significance of these limits for a [D]/[H] ratio is not clear. Another approach is to use measurements of deuterated molecules such as DCN and DCO^+. Penzias (1980) reported tentative detections of DCN and DCO^+. The difficulty here is that isotope exchange reactions cause deuterium to be enhanced in abundance in such molecules by orders of magnitude (see e.g. Wootten (1987)) and consequently, observed abundance ratios such as [DCN]/[HCN] or [DCO^+]/[HCO^+] are not representative of the real D/H ratio. Nevertheless, recent advances in our understanding of interstellar deuterium fractionation (see e.g. Millar et al. (1989)) suggest to us that this approach is worth trying. In this article, we estimate the galactic center deuterium abundance on the basis of new measurements of DCN, DCO^+ and other isotopic species of HCN in the Sgr B2 and Sgr A molecular clouds. An account of the first results of this study was given by Walmsley & Jacq (1990).

2. Observations

The observations were carried out in three sessions between November 1989 and July 1991 using the IRAM 30-m telescope on Pico Veleta. The main characteristics of the telescope are described by Baars et al. (1987). We were able to observe in most sessions using three SIS receivers simultaneously having system temperatures (corrected for telescope efficiency and atmospheric extinction) of 400 K at 3 mm, 550 K at 2 mm, and 1500 K at 1.3 mm respectively. We had available two banks of 500×1 MHz filters and one of these was normally split between 3 and 2 mm. The velocity resolution thus varied between $3.5\,\mathrm{km\,s^{-1}}$ at 3 mm and $2.1\,\mathrm{km\,s^{-1}}$ at 2 mm. A summary of the observed transitions and assumed frequencies is given in

Send offprint requests to: T. Jacq
Correspondence to: jacq@observ.u-bordeaux.fr

Table 1. Angular and spectral resolutions used for different transitions.

Transition	Frequency GHz	HPBW Arc Sec.	Vel. Res. $\mathrm{km\,s^{-1}}$
$HC^{18}O^+$(1-0)	85.162214	29	3.5
$HC^{15}N$(1-0)	86.054961	29	3.5
$H^{13}CN$ (1-0)	86.339944	29	3.5
DCO^+(2-1)	144.077321	17	2.1
DCN (2-1)	144.828109	17	2.1
DCO^+ (3-2)	216.112623	11	1.4
DCN (3-2)	217.238531	11	1.4

Table 1. Pointing checks were carried out on planets (mainly Saturn). We believe that the pointing was accurate to within 5″.

3. Results

We show in Figs. 1 and 2 our spectra in various HCO^+ and HCN isotopomers towards the compact HII region Sgr B2–M (R.A. (1950) = $17^h44^m09.6^s$, Dec(1950) = $-28°22'05.0''$ is position (0,0)). We have detected emission lines of DCN (2-1), DCN (3-2), DCO^+ (2-1), and DCO^+ (3-2) at a velocity of about $60\,\mathrm{km\,s^{-1}}$, which is typical for Sgr B2–M. Line parameters for these deuterated transitions are given in Table 2.

Given the density of spectral lines in Sgr B2–M, there is a non–negligible possibility of a frequency coincidence between the transitions observed by us and lines from other species. In particular, we note the fact that the DCO^+ (3-2) line is likely to be blended with the $19_{2,18}-18_{2,17}$ E and A transitions of methyl formate at 216.1097 and 216.11548 GHz respectively. However, recent BIMA observations (Kuan & Snyder, 1996) have shown that the methyl formate emission in Sgr B2 is concentrated around Sgr B2–N by indeed we detect the $HCOOCH_3$ $29_{9,20}-29_{8,21}$ and $19_{2,18}-18_{2,17}$ at offset (0,+45″) (essentially the Sgr B2–N position). Moreover, the general agreement of the center velocities and line widths given in Table 2 for the DCN (2-1) and DCN (3-2) transitions argues for the correctness of the identification. The DCN and DCO^+ (2-1) line parameters are also consistent with one another. In addition, DCN and DCO^+ are present in several directions (see maps in Figs. 5 and 6). Hence, our results, together with our detection of HDO and NH_2D lines (Jacq et al., 1990) confirm the presence of deuterated species in the galactic center region.

In contrast, for $HC^{15}N$(1-0), $H^{13}CN$ (1-0), and $HC^{18}O^+$ (1-0) we observe a blend of emission and absorption, with the absorption at $\simeq 65\,\mathrm{km\,s^{-1}}$ and the emission at velocities more negative than $58\,\mathrm{km\,s^{-1}}$. In addition for $H^{13}CN$ (1-0), we observe both emission in the velocity range 80-110 $\mathrm{km\,s^{-1}}$, absorption features at 5, -20, and $-40\,\mathrm{km\,s^{-1}}$(Fig. 3). $H^{13}CN$ (1-0) was also observed by Greaves et al. (1992) with the Nobeyama 45 m telescope. Thus there seems to be agreement between these two observations. Clearly, the main absorption component observed in $HC^{15}N$(1-0), $H^{13}CN$ (1-0) and $HC^{18}O^+$is not seen in the deuterated species. In fact, we can put an upper limit (3σ) on the absolute value of the main–beam brightness temperature of an *absorption* line in the line of sight of 0.12 K in DCN(2-1) and of 0.08 K in DCO^+(2-1).

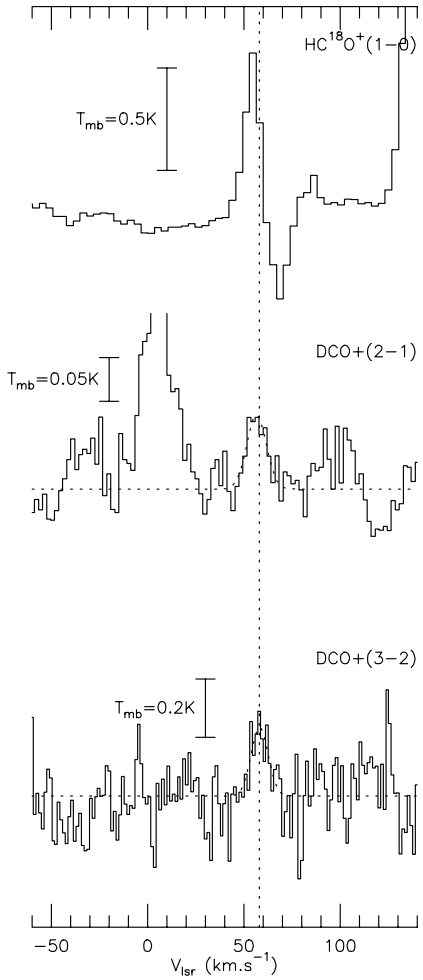

Fig. 1. Spectra of $HC^{18}O^+$(1-0), DCO^+ (2-1), and DCO^+(3-2) towards Sgr B2–M (-15,0)

Table 2. Line parameters of deuterated species towards Sgr B2 (Sgr B2 (0,0) is Sgr B2 Main) and Sgr A. Values in parentheses denote errors and an asterisk implies the value was fixed in the gauss fit. Offsets are in arc seconds.

Transition	Position	Int.Int. $\mathrm{K\,km\,s^{-1}}$	v_{lsr} $\mathrm{km\,s^{-1}}$	Δv $\mathrm{km\,s^{-1}}$
DCO^+ (2-1)	Sgr B2 (-15,0)	1.1(0.2)	56.7(1)	11.8(3)
DCO^+ (3-2)	Sgr B2 (-15,0)	2.6(1)	58.2(2)	10.4(4)
DCN (2-1)	Sgr B2 (0,0)	5.46(1)	59.6(1)	13.9(4)
DCN (3-2)	Sgr B2 (0,0)	4.49(1)	58.0(1)	9.3(3)
DCN (2-1)	Sgr B2 (-15,0)	8.4(0.5)	58.0(0.4)	14.3(1)
DCN (3-2)	Sgr B2 (-15,0)	11.4(2)	58 (*)	14.3(*)
DCN (2-1)	Sgr A	1.9(0.4)	46(2)	18(5)
DCN (3-2)	Sgr A	1.2(1)	43(5)	13(13)

Moreover, the absorption in non-deuterated species makes it difficult to determine the emission profile which would be observed in the absence of absorption. It is presumably this latter entity which is of interest when trying to estimate (for

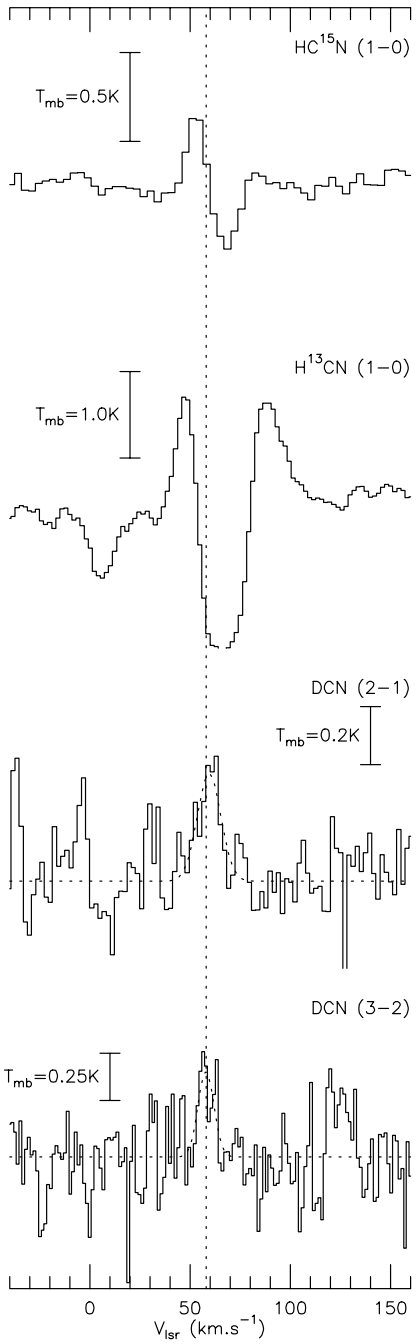

Fig. 2. Spectra of $HC^{15}N$(1-0), $H^{13}CN$ (1-0), DCN (2-1), DCN (3-2) towards Sgr B2–M (-15,0)

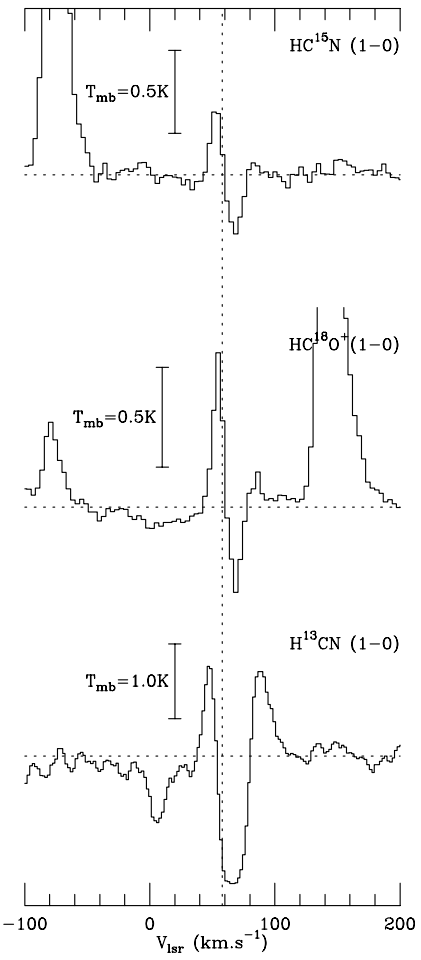

Fig. 3. Spectra of $H^{13}CN$ (1-0), $HC^{18}O^+$ (1-0), and $HC^{15}N$ (1-0) (bottom to top) towards Sgr B2–M showing the negative velocity absorption features

example) the $[DCO^+]/[HC^{18}O^+]$ abundance ratio in Sgr B2–M. We discuss this point further below but note here that this difficulty caused us to observe positions without a continuum background (e.g. Sgr A) in order to be able to better compare deuterated and non–deuterated species.

An interesting by-product of our results is that we observe several absorption components at velocities more negative than $20\,\mathrm{km\,s^{-1}}$ in $H^{13}CN$ (1-0) and $HC^{18}O^+$(1-0). These correspond to features both in the center region and in the 3 kpc arm. The spectra are shown in Fig. 3.

To avoid problems due to absorption in $H^{13}CN$, we observed the spectra towards Sgr A. These profiles are shown in Fig. 4. The position used for Sgr A was (Zylka, 1990) R.A.(1950) = $17^h42^m38.1^s$, Dec(1950)= $-28^\circ\ 58'\ 42.6''$). One sees from Fig. 4 that we detected a feature at the frequency of DCN (2-1) but that we only marginally see evidence for DCN (3-2). Moreover the $H^{13}CN$ (1-0) line which was observed at the same position (integrated intensity $82\pm(0.8)\,\mathrm{K\,km\,s^{-1}}$, velocity $48.6\,\mathrm{km\,s^{-1}}$) is much broader (HPW=$40\mathrm{km\,s^{-1}}$) than the feature which we detect in DCN (2-1). This is probably partially due to the larger beam at 3 mm and partially due to radiative transport effects. Regardless of the explanation, this difference in profile makes the determination of an abundance ratio between DCN and $H^{13}CN$ more difficult.

With a similar objective in mind, we have made small maps of Sgr B2 in several of the transitions discussed above. In Fig. 5, we show maps of the intensity integrated over the velocity range 40 to $80\,\mathrm{km\,s^{-1}}$ in DCN (2-1), DCN (3-2), and $H^{13}CN$ (1-0). The $H^{13}CN$ map is dominated by the absorption towards the two continuum sources Sgr B2–M and Sgr B2–N. The DCN maps show both off-core and extended DCN emission, a trend

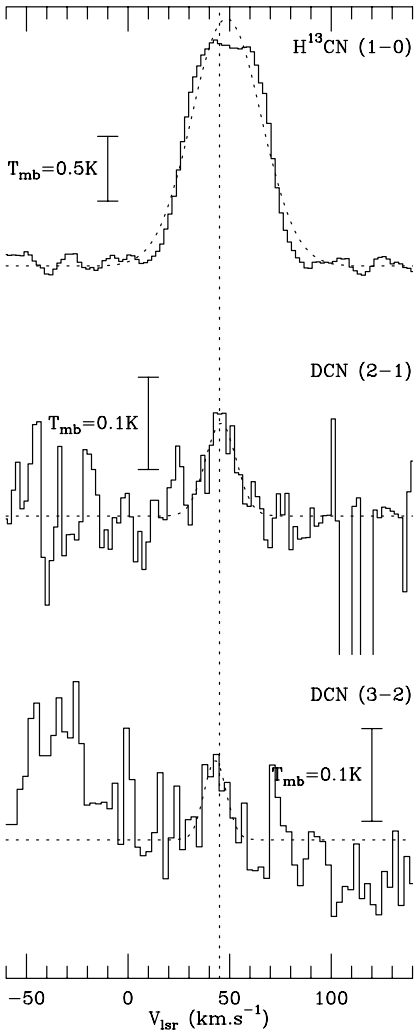

Fig. 4. Spectra of $H^{13}CN$ (1-0), DCN (2-1), and DCN (3-2) towards Sgr A. Dashed profiles are the gaussian fits to the lines

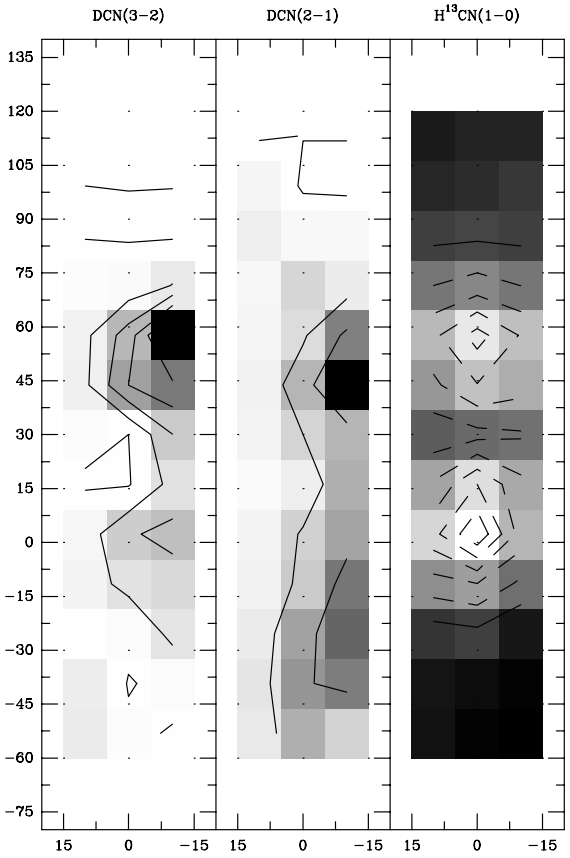

Fig. 5. Contour maps towards Sgr B2–M of integrated intensity over the velocity range 40 to 80 $\mathrm{km\,s^{-1}}$ in DCN (3-2) (left), DCN (2-1) (center), and $H^{13}CN$ (1-0) (right). The three transitions were observed simultaneously. The contour levels are, in K $\mathrm{km\,s^{-1}}$: 0 to 20 by 4, 0 to 16 by 4 and -50 to 0 by 10 respectively. Dashed contours in the $H^{13}CN$ map indicate absorption and by inference denote the positions of the continuum sources Sgr B2 M and N

which has been observed in other hot molecular cores (Hatchell et al. (1998)). Additional data should be obtained to confirm the position offsets between the DCN peaks and the core positions.

The situation for DCO^+ and $HC^{18}O^+$ is in many respects similar to that discussed for the HCN isotopomers. In Fig. 6, we show a comparison of a contour map in $HC^{18}O^+$ with a representation of the integrated intensities of DCO^+ (2-1). The signal-to-noise ratio of the DCO^+ data is not sufficiently high to warrant displaying a contour map for this species. However we note that DCO^+ (2-1) appears to peak away from the Sgr B2–M source at (-15,0).

Finally, we note that our $H^{13}CN$ data are of interest in their own right. In particular, the distribution of the emission at high positive and negative velocities. We show in Fig. 7 the observed intensity distribution in velocity intervals chosen in such a way as to separate the various absorption and emission components. We note for example that the high velocity $H^{13}CN$ (1-0) emission (between 85 and 100 $\mathrm{km\,s^{-1}}$) peaks at offset (0,20) between the Sgr B2–N and Sgr B2–M compact HII regions.

4. Data analysis and determination of column densities

In this section, we consider the profiles which we have observed in $H^{13}CN$, $HC^{15}N$, and $HC^{18}O^+$ towards Sgr B2 and how they can be best compared with the corresponding deuterated species. We then derive column densities at a few selected positions in order to arrive at estimates for the abundance ratios [DCN]/[HCN] and [DCO^+]/[HCO^+].

4.1. Profile analysis for non–deuterated species towards Sgr B2

The relatively complex profiles observed in non–deuterated species towards Sgr B2 requires some discussion. It seems probable to us that these are due to foreground clouds which absorb both the continuum from the HII regions associated with Sgr B2 and the emission lines from the dense gas in the core of Sgr B2. Further we postulate that deuterated species have very low abundances in this foreground absorbing cloud. It is well known (see e.g Hüttemeister et al. 1993) that the gas responsible for much of the absorption in Sgr B2 is at very high temperature (above

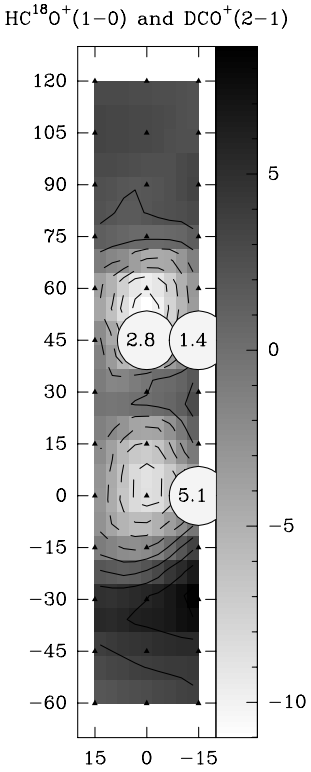

Fig. 6. Comparison of map of $HC^{18}O^+$ (1-0) (grey scale and contours) towards Sgr B2 with values of the DCO^+(2-1) integrated intensity at selected positions. The latter are denoted by the values inscribed within the circles superimposed on the map (2.8 and 1.4 $K km\,s^{-1}$to the North and 5.1 $K km\,s^{-1}$at (-15,0)). We give in both cases the integral of T_B over the velocity range 35-77 $km\,s^{-1}$. Contour units are -12 to 8 by 2 K $km\,s^{-1}$. Contour units are shown on the bar to the right of the map. Dashed contours are negative and show the absorption towards the continuum sources

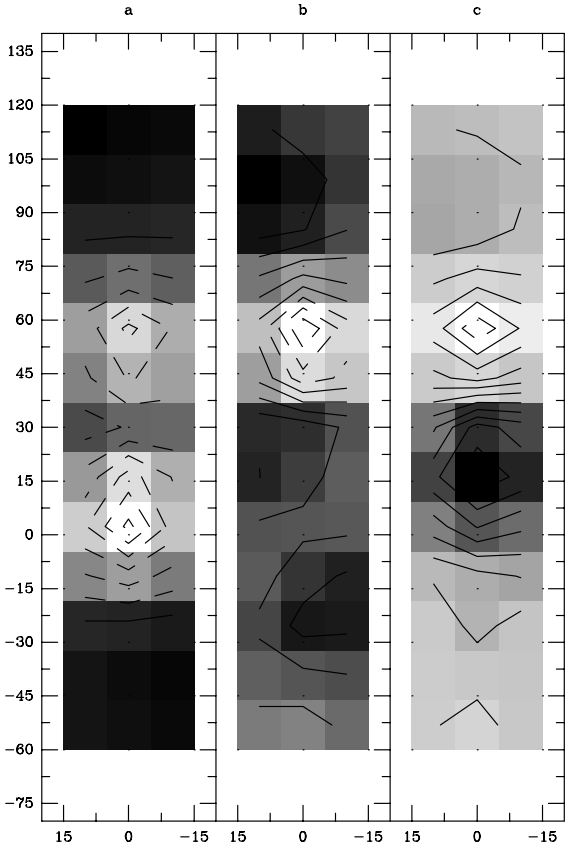

Fig. 7. Map in selected velocity intervals of the $H^{13}CN$ (1-0) integrated intensity (full contours) or absorption (dashed) towards Sgr B2. The left hand panel shows the integrated intensity in the velocity interval 50-80 $km\,s^{-1}$, the center panel in the velocity interval 80-85 $km\,s^{-1}$, and the right hand panel in the velocity interval 85-100 $km\,s^{-1}$. Dashed contours are negative and show absorption towards the continuum sources. Contours are respectively -60 to 10 by 10, -4 to 6 by 1 and -4 to 20 by 2 in K $km\,s^{-1}$

150 K) and it is thus reasonable that there is little or no fractionation in this foreground regions.

On the other hand, the denser gas in the core of Sgr B2 seems likely to have lower temperatures at which considerable fractionation is possible. We therefore may see emission of both deuterated and non–deuterated species from this region. A consequence is that it becomes non–trivial to isolate the emission of species such as $HC^{15}N$ and $H^{13}CN$ which correspond to the observed DCN emission. Similar remarks hold for $HC^{18}O^+$ and DCO^+. We have therefore attempted to fit the $HC^{15}N$ (or $HC^{18}O^+$) profile by an equation of the form:

$$T_l(v) = T_{em}(v)\, e^{-\tau_a(v)} - T_c\,(1 - e^{-\tau_a(v)}) \quad (1)$$

In the above equation, $T_{em}(v)$ represents the line emission from the cloud in the core of Sgr-B2 responsible for both deuterated and non–deuterated line emission. We assume it to have a gaussian profile of amplitude T_e centered at velocity v_e and of half–power width Δv_e, i.e.:

$$T_{em}(v) \;=\; T_e\, e^{(-2.77\,(v-v_e)^2/\Delta v_e^2)}$$

The second term on the right side of Eq. (1) describes the absorption of the continuum radiation of main-beam brightness temperature T_c. The absorption optical depth τ_a is supposed to have a gaussian profile centered at v_a and of half-width Δv_a. Thus, one has:

$$\tau_a \;=\; \tau_a^0\, e^{-(2.77(v-v_a)^2/\Delta v_a^2)} \quad (2)$$

The profile defined by Eq. (1) is capable of approximating the observed $HC^{15}N$(1-0) and $HC^{18}O^+$(1-0) spectra such as those shown in Figs. 1 and 2. However, our objective is to isolate that portion of the $HC^{15}N$ (or $HC^{18}O^+$) profile which corresponds to the observed DCN (DCO^+) emission. Hence, we have carried out fits with v_e and Δv_e fixed and set these equal to the parameters determined for the deuterated species (Table 2). Moreover we also use our knowledge of T_c (1.6 K at 3mm in main-beam brightness units towards (-15,0)) in order to reduce the number of free parameters to 4 (T_e, τ_a^0, v_a, and Δv_a).

In Fig. 8, we show the results of least square fits we have made to the observed profiles at (-15″,0). The corresponding fit parameters are given in Table 3. One sees that there is an adequate fit to our observed $HC^{15}N$(1-0) and $HC^{18}O^+$(1-0) profiles.

Table 3. Line parameters from fit of profile given by Eq. 1 towards (-15,0) offset in Sgr B2.

Transition	T_e K	τ_a^0	v_a km s^{-1}	Δv_a km s^{-1}
$HC^{18}O^+$(1-0)	1.0	1.0	65.9	12.4
$HC^{15}N$(1-0)	2.5	1.0	62.8	15.6

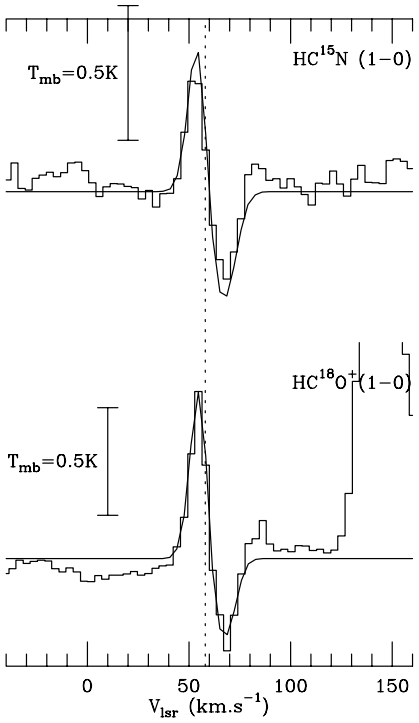

Fig. 8. Profile fits defined by Eqs. 1 and 2 to spectra observed at the (-15,0) offset towards Sgr B2. The corresponding fit parameters are given in Table 3

4.2. Column density estimates towards Sgr B2 and Sgr A

In this section, we estimate column densities for the species of interest towards a few selected positions. We consider first the deuterated species. We consider it likely that the DCN and DCO^+ emission observed by us is optically thin and at transition excitation temperatures considerably larger than the temperature equivalents of the line frequencies. We base this on the weakness of the lines and the high densities and temperatures in the Sgr B2 and Sgr A regions. The column densities in the respective J=2 levels of DCN and DCO^+ are thus:

$$\mathrm{N(DX, J=2)} \;=\; \mathrm{k(X)} \int T_\mathrm{l}(\mathrm{DX}, 2-1)\, dv$$

where X is either CN or CO^+ and k(CO^+) = $1.72\,10^{11}$ and k(CN)= $3.22\,10^{11}$ (k(X) in cm^{-2} (K km s^{-1})$^{-1}$). For this situation, where excitation temperatures are high, the ratio R_{32} of the integrated line intensities in J=3-2 and 2-1 for the two species is:

$$R_{32} = \frac{\int T_\mathrm{l}(\mathrm{DX, J=3-2})\, dv}{\int T_\mathrm{l}(\mathrm{DX, J=2-1})\, dv} \;=\; 2.25\, e^{-(7.0/T_\mathrm{r})}$$

Table 4. Column density estimates for deuterated species towards Sgr B2 and Sgr A. The range of values for $N_{\rm tot}$ corresponds to $T_\mathrm{r} = 10$ and 50 K.

Species	Position	N(J=2) cm^{-2}	$N_{\rm tot}$ cm^{-2}
DCO^+(2-1)	Sgr B2 (-15,0)	$1.9\ 10^{11}$	0.6–1.3 10^{12}
DCN (2-1)	Sgr B2 (0,0)	$1.8\,10^{12}$	6–13 10^{12}
DCN (2-1)	Sgr A (0,0)	$6.1\,10^{11}$	2–4 10^{12}

Here we assume that the emission is extended relative to the beams at 2 and 1.3 mm. The rotation temperature T_r in this equation is unknown but, is expected to be much higher than 10 K in the dense hot medium surrounding Sgr B2–M and Sgr A. Thus from the above equation, one would expect the observed ratios R_{32} to be of order 2; this is the case for DCO^+ (cf Table 2) and thus $T_\mathrm{r} \approx$60 K. Inspection of Table 2 shows that our observed values of R_{32} for DCN are in fact smaller than 1.5. We are not convinced that this is significant, but note here that either the assumption that the emission of the deuterated species is extended or the assumption that excitation temperatures are low may be incorrect. (Formally, the observed DCN intensity ratios suggest that T_r is of order 10-20 K). Higher resolution mapping data are needed to check the spatial structure in the DCN and DCO^+ emissions.

To derive total column densities for DCN or DCO^+, one requires the ratios N(DX)/N(DX,J=2). With the simplifying assumptions discussed above, one expects (due to the accident that the rotational constants only differ by 0.5 percent, one can use the same formula for both species):

$$\mathrm{N(DX)/N(DX, J=2)} \;=\; (T_\mathrm{r}/8.7)\, e^{(10.4/T_\mathrm{r})}$$

In Table 4, we give column densities derived in this way based upon the parameters given in Table 2. We have assumed for this purpose that T_r is between 10 K and 50 K and this is reflected in the uncertainties given in the last column of Table 4.

Of most interest to us are the abundance ratios [DCN]/[$HC^{15}N$] and [DCO^+]/[$HC^{18}O^+$] for which we expect that many of the uncertainties due to excitation cancel out. What we have actually measured are the 2-1 and 3-2 transitions for the deuterated species and the 1-0 transition of the hydrogenated species. We use the same simple assumptions outlined above to derive these quantities. Thus one can write for [DCN]/[$HC^{15}N$] (the same formula with essentially the same numerical constants holds for [DCO^+]/[$HC^{18}O^+$]):

$$\frac{[DCN]}{[\mathrm{HC^{15}N}]} = 0.34\, \exp\left(3.5/\mathrm{T_r}\right) \frac{I(DCN(2-1))}{I(\mathrm{HC^{15}N}(1-0))}$$

Using the above formulae and assuming the $^{14}N/^{15}N$ and $^{16}O/^{18}O$ ratios to be 800 and 250 respectively at the galactic center (Wilson & Rood (1994), Güsten & Ungerechts (1985)), we find for Sgr B2 (-15″,0) [DCN]/[HCN] $\approx 1.1 - 1.4\,10^{-4}$ and [DCO^+]/[HCO^+] = $1.6 - 2.1\,10^{-4}$. The range of values corresponds to T_r = 50-10 K. In order to determine I($HC^{15}N$(1-0)) and I($HC^{18}O^+$(1-0)) we have adopted T_e = 2.5 and 1.0 K,

respectively (see Table 3); these values were determined for $\Delta v_{\rm e}$ equal to the deuterated species line widths. The uncertainty in the ratios [DX]/[HX] is difficult to estimate. It is not very sensitive however to the exact value of $T_{\rm r}$. The largest uncertainty comes from the adopted ^{14}N/^{15}N and ^{16}O/^{18}O ratios. Nevertheless both [DCN]/[HCN] and [DCO^+]/[HCO^+] are similar, and we estimate these ratios to be uncertain by a factor of 2.

Towards Sgr A, the situation is somewhat different because we did not observe $HC^{15}N$ but on the other hand, our results are not compromised by foreground absorption. The likelihood is high that the $H^{13}CN$(1-0) transition observed by us is optically thick. A lower limit to the $H^{13}CN$ column density is $2.3\,10^{14}$ cm^{-2} if one assumes an excitation temperature of 20 K corresponding to $5\,10^{15}$ cm^{-2} in HCN taking ^{12}C/^{13}C =20 from Wilson & Rood (1994) and hence, we can derive an upper limit to [DCN]/[HCN] of $6\,10^{-4}$.

5. Deuterium fractionation in Sgr B2–M (-15,0)

In order to estimate the degree of fractionation of deuterium in the galactic center clouds, we have used the time dependent code of Lee et al. (1996) (see also Caselli et al. (1998)) adapted to the conditions of the Sgr B2 cloud. The galactic center clouds differ from molecular clouds in the disk of our Galaxy in several ways. One of these is that heavy element abundances appear to be in general higher by factors of order 2 (see Shields et al. (1994), Simpson et al. (1995)) than in the solar neighbourhood. A second characteristic is that galactic center clouds in general are hotter and denser than molecular clouds in the disk (see Hüttemeister et al. (1993), de Vicente et al. (1997)). In particular, we note that our detections of DCN and DCO^+ towards Sgr B2 are offset from the main UCHII regions in the complex and likely form in the "warm envelope" which de Vicente et al. (1997) find to vary in temperature between 40 and 120 K. The value towards the (-15″,0) offset seems likely to be of order 100 K but with large uncertainty. The density in the envelope according to these authors is $3\,10^5$ cm^{-3} at a radius of 1 parsec (25″). We will in the following assume that these conditions hold in the region where the DCN and DCO^+ lines observed by us are formed.

A surprising feature of the galactic center clouds is however that despite the differences in physical conditions and abundances mentioned above, the chemical mix found in clouds such as Sgr B2 seems relatively "normal" (see Irvine et al. (1987) for example). Thus, if one considers abundance ratios such as [HCN]/[CO] and [HCO^+]/[CO] for example, they are found in Sgr B2 to be of order $1-2\,10^{-4}$ which is not greatly different from the corresponding ratios found in nearby dust clouds such as TMC1. There is some evidence however (Lis & Goldsmith, 1989) that abundances relative to hydrogen are *lower* than in nearby clouds. Lis and Goldsmith in fact find [$C^{18}O$]/[H_2] to be $5\,10^{-8}$ which corresponds to [CO]/[H_2] = $1.25\,10^{-5}$ (see Wilson & Rood (1994)). This is roughly an order of magnitude less than found in local clouds and since one expects most *gas phase carbon* to be in the form of CO, it suggests considerable depletion in Sgr B2. Chemical abundances (as well as deuterium fractionation) are in general sensitive to depletion (see Caselli et al. (1998)) and this makes it even more surprising that the abundances relative to CO are relatively normal.

We note moreover that the abundances in clouds such as Sgr B2 are unlikely to be in chemical steady state. The regions of interest to us have dimensions of approximately a parsec and velocity dispersions of 5-10 $\rm km\,s^{-1}$ which implies dynamical time scales of order 10^5 years. While they may remain as coherent entities for much longer than that, they are unlikely to have lifetimes longer than one rotation period around the galactic center which for Sgr B2 is of order $3\,10^6$ years. This is somewhat less than the timescales required for the gas phase chemistry to reach a steady state and hence predictions about the chemical make up of regions such as Sgr B2 are dependent on the initial conditions and timescales chosen.

With this in mind, we have carried out calculations of the gas phase chemistry for a time dependent model with a "standard" ionization rate of $1.3\,10^{-17}\,\rm s^{-1}$ and with a reaction network essentially identical to that used by Caselli et al. (1998). In order to treat DCN, we have added 55 reactions (available upon request) treating the deuterated cyanides and related species. We assume that initially hydrogen is molecular and deuterium in the form of HD but all other species are present as atoms (or ions for species with ionization potential below 13.6 eV). We have used in these calculations abundances for both C and N relative to hydrogen of 10^{-5}. We take [S/H] = 10^{-7}, [Si/H] = 10^{-9} and all other heavy element abundances (see Lee et al. (1996)) equal to 10^{-10}. The rationale behind this, as far as carbon is concerned, is to obtain rough consistency with the [CO]/[H_2] result of Lis and Goldsmith mentioned above. Carbon in these calculations becomes transformed into CO and hence the total C abundance defines the final CO abundance. For other elements, the situation is less clear, since the Lis and Goldsmith result suggests that a considerable degree of heavy element depletion has taken place in Sgr B2.

Important for this study is the fact that the gas phase oxygen abundance or the [O]/[C] ratio plays a critical role in the chemistry. It is well known (e.g. Bergin et al. (1997), Terzieva & Herbst (1998)) that the abundances of C-rich species are sensitive to this ratio and we have used this fact to determine [O]/[C]. Irvine et al. give for example in Sgr B2 [HCN]/[CO] and [HCO^+]/[CO] of order 10^{-4}, [NH_3]/[CO] between 10^{-4} and 10^{-3} and [HC_3N]/[CO] =$2.5\,10^{-5}$; we exclude models which differ by more than an order of magnitude from these values. In this way, we have concluded that roughly speaking, the best fit to observed abundances is obtained with [O/C] between 1 and 1.5. We doubt whether this is the actual situation and think it probable in a highly turbulent source such as Sgr B2 that material is being cycled between C-rich areas where grain mantles are returned to the gas phase and C-poor areas where a very large fraction of the heavy elements are depleted out. Within the framework of our model however, we find that we can get a reasonable approximation to observed abundances with [O]/[C]=1.25. N is less critical, but the relatively large [NH_3] abundance suggests that it has a similar abundance to O and C.

We show in Fig. 9 the results of "pseudo time dependent" calculations which we have carried out of the evolution of the gas

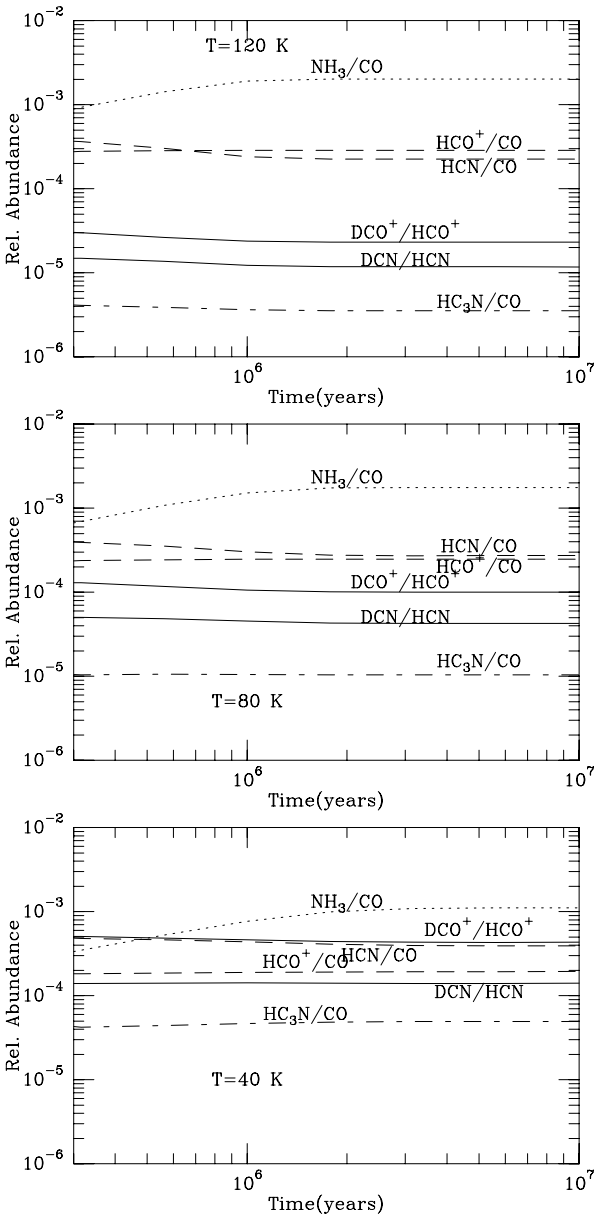

Fig. 9. Relative abundances of [DCN]/[HCN] and [DCO^+]/[HCO^+] (full lines) as functions of time for the pseudo time dependent model discussed in the text. The dashed lines show predictions for the ratios [HCN]/[CO] and [HCO^+]/[CO]. The dotted line shows the behavior of [NH_3]/[CO] and the dash-dot line the dependence of [HC_3N]/[CO]. The top panel shows results for a temperature of 120 K, the center panel for 80 K, and the bottom panel for 40 K. We have assumed a density n(H_2) of $3\,10^5$ cm^{-3} and a D/H ratio of 10^{-6}. We additionally have assumed the ratio of gas phase oxygen to carbon to be 1.25 and the C(N) abundances relative to H to be 10^{-5}

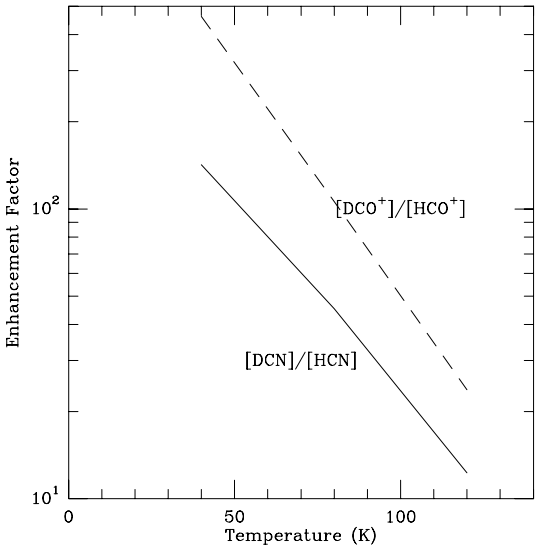

Fig. 10. Computed enhancement of the [DCN]/[HCN] and [DCO^+]/[HCO^+] abundance ratios relative to the total [D]/[H] ratio as function of kinetic temperature

phase chemistry for conditions appropriate for Sgr B2 assuming D/H = 10^{-6} as suggested later. We show results for T=40, 80 and 120 K and the above abundance mix. One sees that although it takes several million years to achieve steady state, the ratios [DCN]/[HCN] and [DCO^+]/[HCO^+] are not particularly time dependent. However, they are sensitive to temperature as one might expect (see Millar et al. (1989)) since the important deuterium enrichment reactions have barriers of up to 550 K.

6. Estimate of the true D/H ratio and constraint on astration model

Fig. 10 shows the computed enhancement ratios f_{en}(DCN) and f_{en}(DCO^+) (by which we define the ratio ([DCN]/[HCN])/$(D/H)_{tot}$ and similarly for DCO^+) as a function of temperature. f_{en}(DCN) varies between 140 and 12 as the temperature varies from 40 to 120 K. The analogous ratio for DCO^+ varies between 460 and 23 over the same temperature range. In Sect. 4, we showed that our observations of Sgr B2 imply [DCN]/[HCN] $\simeq 1.1 - 1.4\,10^{-4}$ and [DCO^+]/[HCO^+] $\simeq 1.6 - 2.1\,10^{-4}$. These ratios imply a total relative deuterium abundance of $8\,10^{-7} - 10^{-5}$ and $3.5\,10^{-7} - 9\,10^{-6}$ corresponding to the kinetic temperature range 40 to 120 K. Combining the arithmetic means of these intervals for both species, we conclude that the best estimate which we can make is that $(D/H)_{tot}$ is of order $5\,10^{-6}$ but there is an order of magnitude uncertainty.

In some ways our results for the Sgr A cloud are less uncertain; we have an upper limit on [DCN]/[HCN] of $6\,10^{-4}$. Zylka (1990) estimates that at the position observed by us, the temperature (from methyl acetylene) is 70 K, the H_2 column density is $3\,10^{23}$ cm^{-2}, and the H_2 number density is $2\,10^5$ cm^{-3}. As above, we estimate f_{en}(DCN) to be 60 and hence one has an upper limit on $(D/H)_{tot}$ of $1.0\,10^{-5}$. Thus our result for Sgr A like that for Sgr B2 suggests a deuterium abundance lower than in the solar neighbourhood where D/H is of order $2\,10^{-5}$.

However the uncertainties are large. These stem both from the uncertainty on the temperature in the region where the deuterated species are observed and the general uncertainties in galactic center chemistry. While it might be possible to reduce

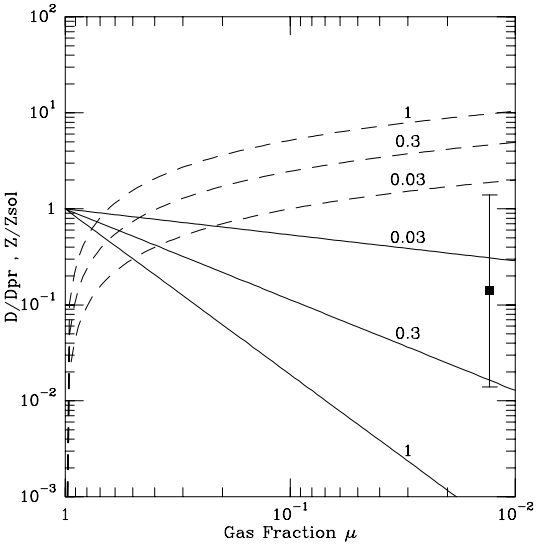

Fig. 11. Computed variation of the deuterium abundance (continuous lines) as a function of the fractional mass in gas μ using the simple analytical model discussed by Galli et al. (1995). Results are given for model Initial Mass Functions with lower mass cut offs at 0.03 (standard), 0.3, and 1 $M_\odot$. The black square represents our estimate of the D abundance based upon our Sgr-B2 measurements for $\mu \approx 0.01$. The error bar corresponds to one order of magnitude uncertainty. It should be noted that the error on the galactic center value for μ is at least a factor of 2. The dashed lines show the metal abundance Z

the latter by attempting to "fit" the abundances of a larger number of species, it is clear that we are limited by the fact that there are likely to be large temperature gradients across the regions observed by us. Additionally, there are the observational uncertainties in determining the [DCN]/[HCN] or [DCO^+]/[HCO^+] ratios in Sgr B2 referred to previously. However, we conclude from this that our results are consistent with a ratio [D/H] of order $5\,10^{-6}$ in Sgr B2 to within an order of magnitude. Certainly, the model results presented here make it seem unlikely that f_{en}(DCN) defined above is larger than 1000 and this allows us to put a firm lower limit on the deuterium abundance of 10^{-7}. These small values are certainly consistent with previous upper limits.

If one takes a standard model for the astration of deuterium (Galli et al., 1995), one finds that the D-abundance [D/H] can be expressed in terms of the ratio of interstellar gas mass to total mass μ and the mean mass fraction returned to the gas (i.e. not lost in a remnant) subsequent to stellar evolution R. One finds with reasonable accuracy:

$$[\mathrm{D}]/[\mathrm{H}] \;=\; ([\mathrm{D}]/[\mathrm{H}])_{\mathrm{pr}}\, \mu^{R/(1-R)} \qquad (3)$$

Here $([\mathrm{D}]/[\mathrm{H}])_{\mathrm{pr}}$ is the primordial D mass fraction which we take to be $3.5\,10^{-5}$ based on the discussion of Galli et al. (1995). They also estimate that with a standard IMF, R is 0.21 from which one concludes that $[D]/[H]$ behaves roughly as $\mu^{.27}$. Fig. 11 shows predictions for cases where the IMF has a lower mass cut off of 0.03 (standard), 0.3 and 1 $M_\odot$ respectively. The ratio μ of gas to stars by mass is thought to be of order 0.01 in the galactic center (Güsten, 1989) as compared to 0.1 in the solar neighbourhood and we have used this fact to place our observed [D]/[H] estimate (0.14 in $(D/H)_{\mathrm{pr}}$ units) in Fig. 11. We also show in Fig. 11 the expected behavior of the metal abundance Z with mass fraction.

From this, one concludes that our observed $[D]/[H]$ ratios are compatible with a large variation in the IMF but we can exclude the possibility that the lower mass cut–off to the IMF is as high as 1 $M_\odot$. Current estimates of the metal abundance, for example, probably rule out values higher than 5 times solar and this would confine (see Fig. 11) the lower mass cut off to values lower than 0.3 $M_\odot$. Moreover, measurements of the He abundances (in particular ^{3}He, see Balser et al. (1994)) also give approximate constraints on the star formation history. Nevertheless, the uncertainties in all these techniques is large and (if one can improve fractionation estimates) the deuterium abundance offers a useful independent test of evolution theories.

7. Conclusions

The results presented confirm the observation of Penzias (1980) and Jacq et al. (1990) that deuterated molecules are present at a low level in the galactic center molecular clouds. They also show that these species are not present in the hot absorbing layer seen towards Sgr B2 where presumably fractionation is completely absent. This circumstance has the consequence that, in Sgr B2, single dish measurements of the [DCN]/[HCN] and/or [DCO^+]/[HCO^+] ratios are rendered difficult due to the complexities of radiative transfer and geometry in Sgr B2. The solution to this problem which we have adopted is not ideal and we recommend that future studies of this problem should be concentrated on positions such as that towards Sgr A where no strong absorption in HCN is present. We note also that our main uncertainty is that we have only crude estimates of the physical parameters (in particular the temperature) in the region where the observed DCN and DCO^+ lines form. New measurements of the DCN (DCO^+) excitation would considerably help in reducing this uncertainty.

We conclude that, to within an order of magnitude, the ratio of [D/H] in Sgr B2 is $5\,10^{-6}$. This is roughly a factor 10 less than in the solar neighbourhood. This is a surprisingly low value. If so, it suggests that [D/H] varies from $4\,10^{-5}$ in the outer Galaxy (Chengalur et al., 1997) to $5\,10^{-6}$ near the center.

We have also used our D/H measurement in Sgr B2 to derive an estimate of $([\mathrm{D}]/[\mathrm{H}])/([\mathrm{D}]/[\mathrm{H}])_{\mathrm{pr}}$ which seems to exclude a lower mass cut-off to the IMF as high as 1 $M_\odot$.

Acknowledgements. Thanks are due to Eric Herbst for the use of his pseudo time-dependent chemistry code and to Daniele Galli for his comments on deuterium astration. MW acknowledges travel support from ASI grant ARS 96-66 and CNR grant 97.00018.CT02.

References

Baars J.W.M., Hooghoudt B.G., Mezger P.G., De Jonge M.J., 1987, A&A 175, 319

Balser D., Bania T., Brockway C., Rood R., Wilson T., 1994, ApJ 430, 667

Bergin E., Goldsmith P., Snell R., Langer W., 1997, ApJ 482, 285
Boesgaard A.M. Steigman G., 1985, ARA&A 23, 319
Caselli P., Walmsley C., Terzieva R., Herbst E., 1998, ApJ 499, 234
Chengalur J., Braun R., Burton W., 1997, A&A 318, L35
de Vicente P., Martin-Pintado J., Wilson T., 1997, A&A 320, 957
Galli D., Palla F., Ferrini F., Penco U., 1995, ApJ 443, 536
Greaves J.S., White G.J., Ohishi M., Hasegawa T., Sunada K., 1992, A&A 260, 381
Güsten R., 1989, In: Morris M. (ed.) The Galactic Center. p. 89
Güsten R. Ungerechts H., 1985, A&A 145, 241
Hatchell J., Millar T., Rodgers S., 1998, A&A 332, 695
Heiles C., McCullough P.R., Glassgold A.E., 1993, ApJS 89, 271
Huettemeister S., Wilson T.L., Bania T.M., Martin-Pintado J., 1993, A&A 280, 255
Irvine W.M., Goldsmith P.F., Hjalmarson A., 1987, In: Hollenbach H.D.J. (ed.) Interstellar Processes. Reidel, p. 561
Jacq T., Walmsley C.M., Henkel C., et al., 1990, A&A 228, 447
Kuan Y.-J., Snyder L. E., 1996, ApJ 470, 981
Lee H.-H., Bettens R., Herbst E., 1996, A&AS 119, 111
Linsky J.L., Brown A., Gayley K., et al., 1993, ApJ 402, 694
Lis D., Goldsmith P., 1989, ApJ 337, 704
Lubowich D.A., Anantharamaiah K.R., Pasachoff J.M., 1989, ApJ 345, 770
Millar T.J., Bennett A., Herbst E., 1989, ApJ 340, 906
Pasachoff J.M., Vidal-Majar A., 1989, Comments on Astrophys. 14, 61-68
Penzias A.A., 1980, Sci 208, 663
Shields J.C., Ferland G.J., 1994, ApJ 430, 236
Simpson J.P., Colgan S.W.J., Rubin R.H., et al., 1995, ApJ 444, 721
Terzieva R., Herbst E., 1998, ApJ 501, 207
Terzieva R. and Herbst E., 1998,
Walmsley C., Jacq T., 1990, In: Haschick P.A. (ed.) Proceedings of 1990 Haystack Conference
Wilson T., Rood R., 1994, ARA&A 32, 191
Wootten A., 1987, In: Vardya T.S.(ed.) IAU Symposium 120, p. 311
Zylka R., 1990, Ph.D. Thesis, Univ. of Bonn